Stability of Cold Cathode Fluorescent Lamps Driven by Piezoelectric Transformers

Sam Ben-Yaakov, Mor Mordechai Peretz, and Simon Lineykin
Power Electronics Laboratory
Department of Electrical and Computer Engineering
Ben-Gurion University of the Negev
P.O. Box 653, Beer-Sheva 84105, ISRAEL.
Phone: +972-8-646-1561; Fax: +972-8-647-2949;
Email: sby@ee.bgu.ac.il; Website: www.ee.bgu.ac.il/~pel

***Abstract*— The concept of Envelope Impedance (EI) was used to develop a systematic and simple approach for studying the conditions for stability of PT-CCFL systems. It was found that the EI of PTs includes minimum points at low frequency when the EI of the CCFL is negative. This causes the Loop Gain of the system to encircle the –1 point, making the system unstable. The proposed analytical approach could be helpful in sorting out possible remedies for the PT-CCFL instability problems.**

***Keywords*—Piezoelectric transformer, Cold Cathode Flourescent Lamp (CCFL), envelope impedance.**

I. INTRODUCTION

Piezoelectric transformers (PT) are a practical solution for driving Cold Cathode Fluorescent Lamps (CCFL). It has been observed however, that the PT-CCFL system may become unstable (Fig. 1) causing light flickering and high voltage and current stresses. This has been studied in previous works by small signal analysis [1, 2]. A different approach, based on the envelope impedance analysis, was applied previously to study the interaction between conventional HF electronic ballasts and hot cathode fluorescent lamps. The objective of this study was to apply the envelope analysis method to investigate the stability issue of the PT-CCFL system.

II. THE "ENVELOPE IMPEDANCE" CONCEPT

To illustrate the importance of envelope behavior of the PT-CCFL system, we first consider the case of a CCFL driven by a conventional HF ballast (Fig. 2). Assume that V_{in} (Fig. 2) is an adjustable AC source that keeps the rms lamp current constant. By this, the lamp will always be at the same rms operating point. Consider now two cases, one in which the source frequency is very high and the other in which the source frequency is close to the resonance of L_s, C_s. It is clear intuitively and observed experimentally that the system will be stable when driven at very high frequency but unstable when driven at the close to the (L_s, C_s) resonant frequency, f_r. This is because at high frequency, the CCFL sees a current source (high impedance of the inductor) while at the resonant frequency it sees a voltage source, which will render the system unstable [3]. This virtual experiment shows that in the case of non-linear carrier-driven system, stability is not just a network attribute but it depends on the carrier frequency. That is, the same system will be stable for one carrier frequency but unstable for another. This is in contrast to linear feedback systems in which stability is a characteristic of the system and independent of the excitation. Furthermore, in this case stability conditions are not only dependent on the magnitude of the excitation (which sets the operating point) but also on the frequency of the carrier. For the given example, the crucial stability parameter is the Envelope Impedance (EI) that is defined here as the ratio of the envelope of the voltage, to the envelope of the current, when the network is driven by an AM modulated signal (Fig. 3).

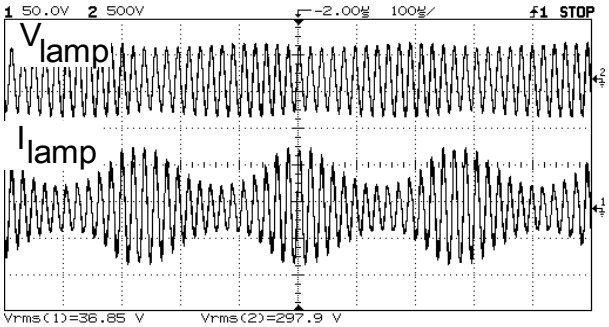

Figure 1. Measured CCFL (JKL BF3250-20B) voltage (0.5KV/Div) and current (3.3mA/Div) under unstable conditions when driven by a PT(ELECERAM ELM-610). Horizontal scale 0.1mS/Div. Carrier frequency: 54 KHz.

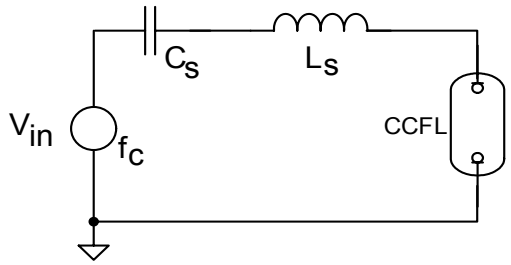

Figure 2. A CCFL driven by a HF resonant ballast.

This research was supported by THE ISRAEL SCIENCE FOUNDATION (grant No. 113/02) and by the Paul Ivanier Center for Robotics and Production management.

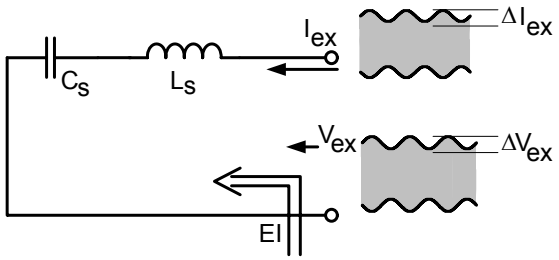

Figure 3. Illustrative explanation of the Envelope Impedance (EI) concept: $EI(f)=\{\Delta V_{ex}/\Delta I_{ex}\}(f)$

It should be noticed that the EI is, in general, a complex number, that is a function of the modulating signal frequency and the carrier frequency, f_c. The carrier frequency can be considered in this case as the "bias point", whereas the modulating frequency, f_m, as the "signal frequency".

Following the above intuitive observation, we consider next the nature of the EI for the example on hand: the resonant ballast (Fig. 3). When the network is driven by an AM modulated signal, the signals involved are the carrier frequency (f_c) and the two side bands: (f_c - f_m) and (f_c + f_m). For a given network with a resonant frequency f_r, then the expected EI as a function of the modulating frequency f_m, for a given carrier frequency f_c, can be guessed by considering the plot of Fig. 4. It shows the impedance of the resonant network (Z_b) as a function of frequency, the location of the carrier frequency f_c and the frequencies of the sidebands. Fig. 4 implies that when $f_m = f_c - f_r$ one would expect to see a valley in the EI. It should be noticed that the valley is located at a frequency that could be substantially lower than f_c or f_r.

III. Stability Criterion

Following [3], we can consider the PT ballast system (Fig. 5) as a feedback loop (Fig. 6). It should be noticed however that, to be consistent with the above observations, the relevant impedances for both systems are their EIs. ZE_{PT} is the EI of the PT and ZE_{lamp} is the EI of the lamp. The stability of this system can thus be studied by analyzing the loop gain (LG) of the feedback loop [3]:

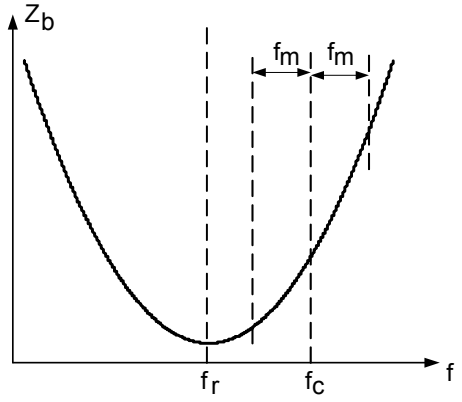

Figure 4. Impedance of a series resonant network, carrier frequency, and side bands.

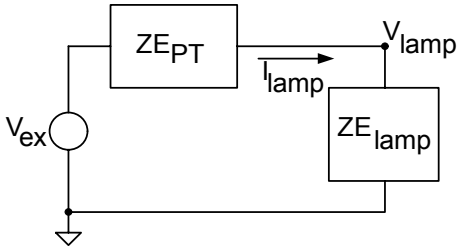

Figure 5. Simplified PT-CCFL ballast system.

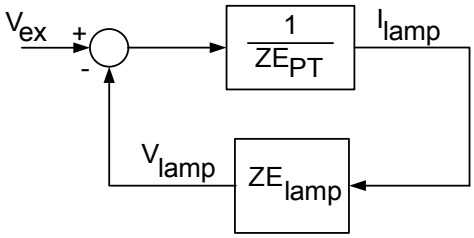

Figure 6. PT-CCFL ballast system represented as a feedback loop.

$$LG = \frac{ZE_{lamp}}{ZE_{PT}} \tag{1}$$

A convenient stability test is the Nyquist Criterion that can be easily applied when the analysis is carried out by simulation [3].

IV. The EI of the PT and the CCFL

It has been shown [4] that the EI of the CCFL (ZE_{CCFL}) for a given operating point can be approximated by the function:

$$ZE_{CCFL} = R_s \frac{\frac{jf_m}{f_p} \cdot \frac{R_{eq}}{R_s} - 1}{\frac{jf_m}{f_p} + 1} \tag{2}$$

where, R_{eq} is the high frequency resistance of the lamp at the operation point, R_s is a constant of the lamp obtained from static set of V-I measurements of the CCFL [4], $f_p = 1/(2\pi \cdot R_1 C_1)$ is the relaxation time constant of the plasma and f_m is the modulation frequency.

At low modulating frequency ($f_m \to 0$) the ZE_{CCFL} is negative ($-R_s$) while at high frequencies ($f_m \to \infty$) the EI is positive. A convenient way to plot the EI is by running a simulation on a behavioral model of the CCFL [4]. A typical EI plot (of the experimental CCFL) is depicted in Fig. 7. It shows that the EI of the CCFL is negative at low frequencies and becomes positive at high frequencies.

Applying envelope simulation [5-8], the EI of the PT as a function of the modulating frequency can be easily obtained. A typical plot (of the experimental PT) is shown in Fig. 8. The

plot can be better understood by comparing it to the (conventional) output impedance of the PT (Fig. 9). The comparison between the plots shows that the minimum values of the EI in Fig. 8 are located at modulating frequencies of 2.5 KHz and 0.5 KHz which are equal to the difference between the carrier frequencies (49 KHz and 51 KHz respectively) and the resonant frequency: 51.5 KHz.

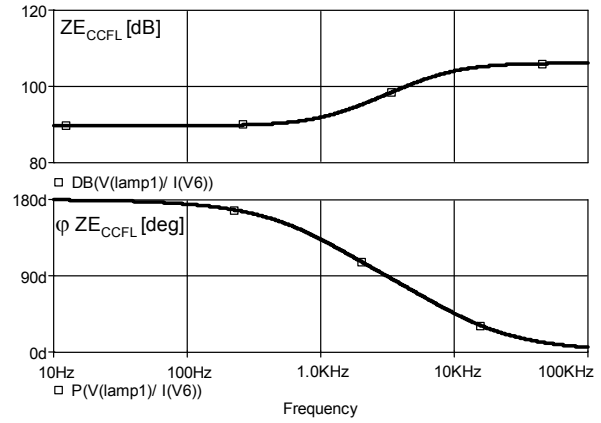

Figure 7. Envelope Impedance of experimental CCFL (JKL BF3250-20B).

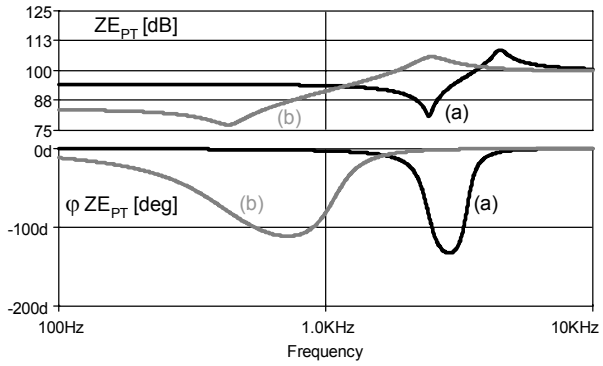

Figure 8. Envelope Impedance of experimental PT (ELECERAM ELM-610) for two carrier frequencies: (a) Operation far from output impedance resonance of the PT f_c=49 KHz and (b) Operation near resonance f_c=51 KHz. (f_r=51.5 KHz)

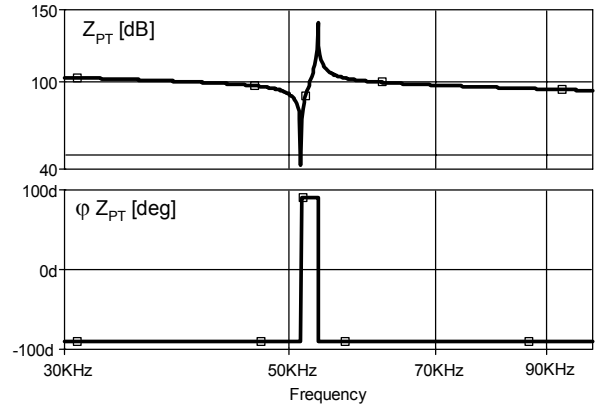

Figure 9. Output impedance of experimental PT.

V. EXPERIMENTAL

A. Extraction of the PT model parameters

The PT was a multilayer Rosen type transformer (ELECERAM ELM-610). The objective of the parameter extraction procedure was to estimate the values of the elements of the PT equivalent circuit (Fig. 10) around the operating frequency of the element (53kHz). The parameters extraction approach adopted in this study is similar to the one described earlier [9] for extracting the terminal impedance of a piezoelectric resonant blade. The difference between the procedure used here and the earlier one is the number of parameters that need to be extracted. In the PT case, two extra parameters are included in model: the transfer ratio of 'transformer' (the two coupled dependent sources) and the output capacitance (C_o, Fig. 10). The extraction procedure was based on some advanced PSpice (Cadence, USA) Version 10 features: a frequency domain data-driven behavioral source (EFREQ), and the PSpice optimization tool.

A1. Reference measurement. The first stage of the extraction procedure was measuring the input to output transfer ratio (TR) of the PT. This was done, in present work, by a network analyzer (HP4395A) coupled to a power amplifier to allow high voltage excitations [10] (Fig. 11). The results were saved as a table file that includes the information of magnitude and phase for each frequency point over the measurement range (48KHz to 60KHz) that was chosen to be around the peak of TR response.

A2. Emulating the measurement in PSpice. The table obtained from the TR measurement was inserted into a PSpice EFREQ behavioral dependent source [9] (Fig. 12) to create a subcircuit that emulates the measured TR of the PT. This source generates a voltage that is a function of a PSpice 'expression' multiplied by a discrete table defined in the frequency domain. In present case, the 'expression' of the EFREQ (Fig. 12) is (V (%IN+, %IN-)), which denotes the input voltage to the element. When a unity AC voltage source is fed to this behavioral source, its output voltage will duplicate the measured TR of the experimental PT.

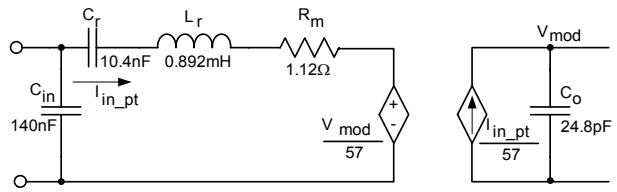

Figure 10. PT equivalent circuit and parameters.

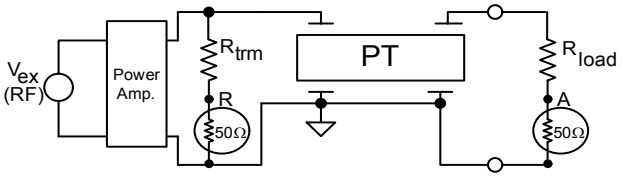

Figure 11. Experimental setup for input to output voltage transfer ratio measurements. The ratio A/R was measured by a network analyzer (HP4395A).

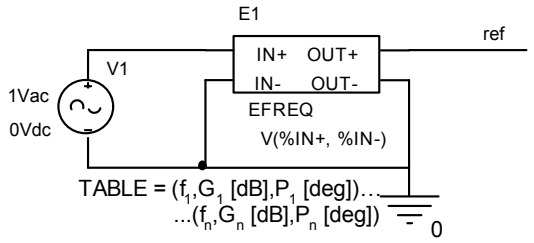

Figure 12. PSpice emulator of experimental TR of the PT. The table of the EFREQ dependent source lists the measured TR (magnitude and phase) over the measured frequency range.

A3. PSpice (Cadence) optimization tool [11]. This add-on package allows the selection of the values of some circuit components to meet a specific goal function. The initial data that are fed to the optimizer include expression of the goal function, additional constraints, if any, and initial values of the components to be optimized.

The objective of the optimization procedure used in this study was to find values of the parameters depicted in Fig. 10 such that they would faithfully represent the experimental PT. This was accomplished by running a set of AC simulations that include the equivalent PT model (Fig. 10) and the EFREQ (Fig. 12), each fed by a unity AC voltage source, and letting the optimizer choose the values of the PT model that will minimize a least square error function. The err goal function was defined by:

$$\mathrm{err} = \left[\mathrm{dB}(V_{\mathrm{ref}}) - \mathrm{dB}(V_{\mathrm{mod}})\right]^2 \times 100 + \left[\mathrm{P}(V_{\mathrm{ref}}) - \mathrm{P}(V_{\mathrm{mod}})\right]^2 \quad (3)$$

The fitting objective:

$$1 \le \mathrm{err} \le 10$$

for:

$$50\mathrm{KHz} \le f \le 56\mathrm{KHz}$$

where 'dB' and 'P' designate decibel and phase operators, V_{ref} is the output voltage of the EFREQ behavioral source (Fig. 12) and V_{mod} is the output voltage of the PT model (Fig. 10). The 100 factor in (3) is used to increase the sensitivity of the error function to gain discrepancies.

The fitting was carried out around a narrower frequency range (50KHz to 56KHz) to improve the accuracy near the TR peak.

The initial values of the model components, needed as an input to the optimization routine, were obtained from two short-circuit (SC) impedance measurements (input SC and output SC). The parameters of the SC measurement were extracted by the fitting routine imbedded in the analyzer, using the HP16092A impedance test kit that was connected to the HP4395A network analyzer.

The estimated values of the PT's model parameters are given in Fig. 10, and the comparison between the measured TR (EFREQ) and model calculated (optimized) TR is depicted in Fig. 13. The observed discrepancies are probably due to the non-linear nature of the PT, when driven by high voltage excitations [10]. However, these differences are negligible within the frequency range (50KHz to 56KHz) of interest.

An experimental measurement of the PT's EI was taken at a carrier frequency of 49 KHz, 2.5 kHz off the resonance frequency of the PT (f_r=51.5 KHz). The EI measurement was carried out by subjecting the PT to an AM modulated signal at the output while its input terminals were shorted. The EI (magnitude and phase) was measured as a function of the modulating frequency (f_m from 0 to 5 KHz). The measured EI (Fig. 14) has its minimum at 2.5 KHz, which is exactly the frequency difference between f_c and f_r. The results are in a very good agreement (magnitude and phase wise) with the envelope simulation (Fig. 14) that was carried out on the PT model using the parameters values that extracted by the proposed procedure.

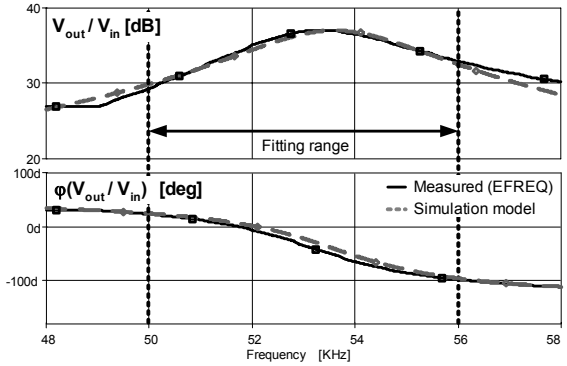

Figure 13. Comparison between measurement result (solid) and optimized model (dashed) input to output TR of experimental PT.

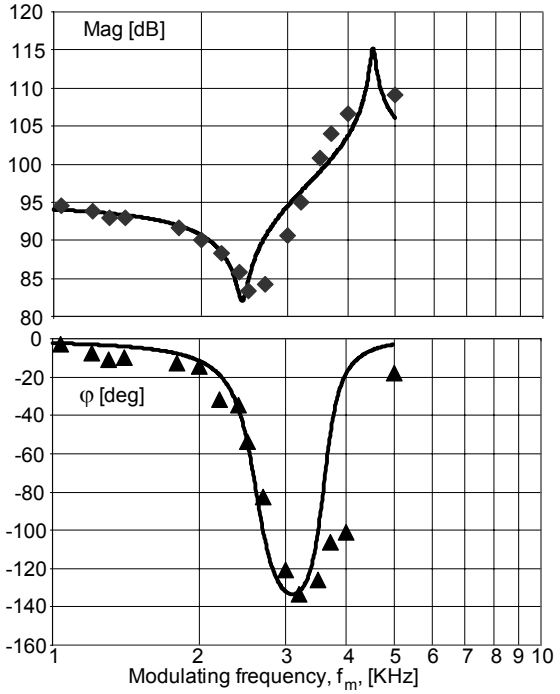

Figure 14. Measured (symbols) and simulated (solid lines) magnitude and phase EI of experimental PT (ELECERAM ELM-610). Carrier frequency: 49 KHz, resonant frequency: 51.5 KHz.

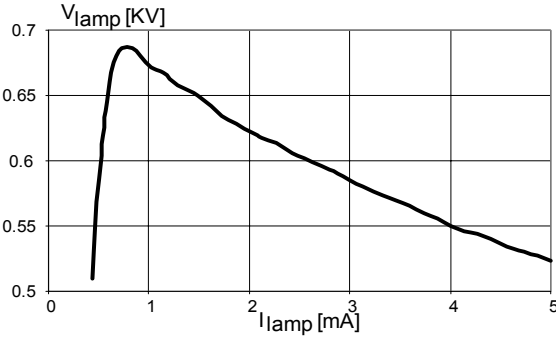

Figure 15. Measured static V-I curves of experimental CCFL (JKL BF3250-20B).

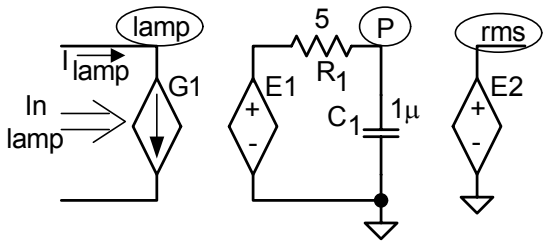

Figure 16. CCFL behavioral model.

B. CCFL model extraction procedure

The experimental CCFL (JKL BF3250-20B) was of 3.2mm diameter, 250mm long, 5mArms nominal current and 520Vrms nominal voltage The static V-I curve of the experimental lamp is given in Fig. 15. Fig. 16 shows the SPICE-compatible model of the experimental CCFL [3, 4].

In this model the lamp is represented as a dependent current source (G_1, Fig. 16) that emulates a variable resistance.

$$G_1 = \frac{V(lamp)}{\frac{730}{V(rms)} + 4.06 \cdot 10^6 \cdot V(rms) - 61.1 \cdot 10^3} \quad (4)$$

where V(lamp) is the lamp rms voltage, and V(rms) is a voltage that emulates the rms lamp current. The denominator of (4) represents the CCFL equivalent resistance curve obtained by fitting the template of (4) to the static lamp resistance derived from the V-I curve of Fig. 15 [4].

The output of the dependent voltage source E_1 (Fig. 16) is proportional to the square of the lamp current {i(lamp)}.

$$E_1 = \{i(lamp)\}^2 \quad (5)$$

The output voltage of E_1 is then passed thru a low-pass network (R_1, C_1, Fig. 16) to extract the low frequency components [4]. The average voltage of C_1 (node 'p' in Fig. 16) is thus a smoothed value of the square rms current. The filtered rms current is then obtained by E_2 (node 'rms' in Fig. 16) as the square root of V(p).

$$E2 = \sqrt{V(p)} \quad (6)$$

The time constant R_1C_1 is chosen by matching the Envelope response of the model to experimental results. This is done, in present study, by subjecting the PT-CCFL system to a HF carrier that is FM modulated. This will cause an AM modulated signal at the lamp terminals due to the PT equivalent series inductance (L_r, Fig, 10) [12, 13]. The CCFL current and voltage traces were then recorded for several modulating frequencies to obtain its EI. The time constant R_1C_1 is then adjusted by matching the model simulated results to the measured response. Fig. 17 shows the measured EI of experimental CCFL compared with the results of the CCFL SPICE model of Fig. 16.

The CCFL and the PT models were examined by envelope simulation to obtain their EI as a function of the modulating frequency (Figs. 7, 8). The data were then used to generate Nyquist plots. Typical Nyquist plots of the experimental PT-CCFL LG are shown in Figs. 18 for different operating conditions.

VI. Results and Discussion

The simulation results clearly point to the fact that the PT-CCFL systems could reach instability under various operating conditions. Prone to instability is the low current range since the incremental impedance (slope of the V-I curve Fig. 15)

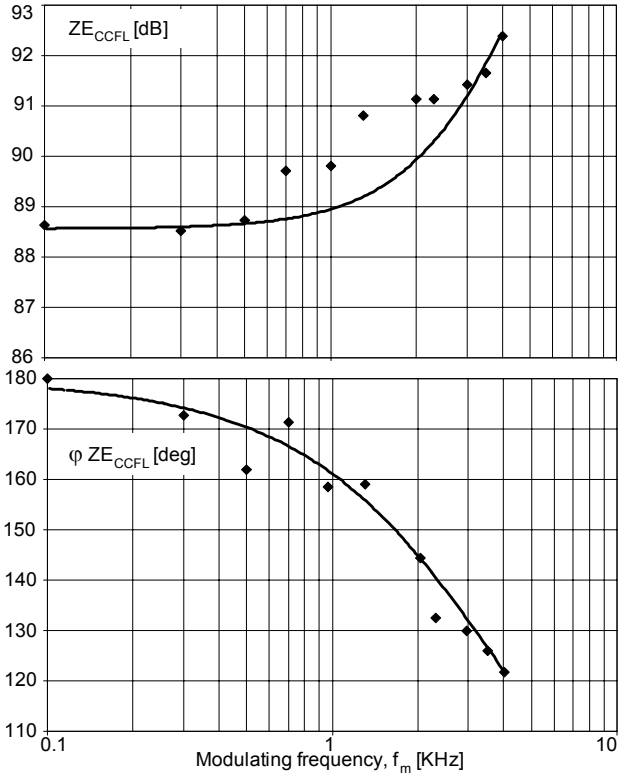

Figure 17. Measured (symbols) and simulated (solid lines) magnitude and phase EI of experimental CCFL (JKL BF3250-20B).

represents a larger negative resistance. However, the real culprit that causes instability is the PT. The expression of the LG (1) implies that instability is reached when the loop gain at low frequency will be negative and smaller than –1 (to encircle the –1 point). The negative sign is due to ZE_{lamp} but the magnitude of the LG depends on the magnitude of ZE_{PT} at low frequencies. Instability is expected when the magnitude of the PT's EI is small.

That is, the system may become unstable when the carrier frequency is close to the resonant frequency of the "mechanical" branch L_r, C_r (Fig. 8). This series resonance network makes, in fact, the PT a poor element for driving CCFLs from the stability point of view.

VII. CONCLUSIONS

The concept of Envelope (EI) Impedance was applied to develop a systematic and simple approach for studying the conditions for instability of PT-CCFL systems. It was found that the EI of PTs, seen at the output terminals, includes a minimum point at low frequency. This minimum is located at a frequency that is equal to the difference between the resonant frequency of the output impedance of the PT and the carrier frequency. Since the EI of the CCFL is negative at low frequencies, the LG of the system will become negative. If the value of the LG gets to be smaller than -1 it will cause the Nyquist plot to encircle the –1 point and hence cause instability due to the existence of a pole at the right half side of the complex plane. The proposed analytical/simulation approach could be helpful in sorting out possible remedies for the PT-CCFL instability problem.

REFERENCES

[1] C. D Wey, T. L. Jong and C. T. Pan, "Design and analysis of an SLPT-based CCFL driver", *IEEE Trans. Industrial Electronics*, 50, 1, 208-217, 2003.

[2] G. Spiazzi, S. Buso, "Small-signal analysis of cold cathode fluorescent lamp ballasts", *IEEE Power Electronics Specialists Conference, PESC-2005*, 2783-2789, Recife, 2005.

[3] S. Glozman, and S. Ben-Yaakov, "Dynamic interaction analysis of HF ballats and fluorescent lamps based on envelope simulation". *IEEE Trans. Industry Applications*, 37,5,1531-1536, 2001.

[4] S. Ben-Yaakov, M. Shvartsas, and S. Glozman, "Statics and dynamics of fluorescent lamps operating at high frequency: modeling and simulation", *IEEE Trans. Industry Applications*, 38, 6, 1486-1492, 2002.

[5] S. Ben-Yaakov, S. Glozman, and R. Rabinovici, "Envelope simulation by SPICE-compatible models of linear electric circuits driven by modulated signals". *IEEE Trans. Industry Applications*, 37, 2, 527-533, 2001.

[6] S. Lineykin and S. Ben-Yaakov, "A unified SPICE compatible model for large and small signal envelope simulation of linear circuits excited by modulated signals", *IEEE Power Electronics Specialists Conference, PESC-2003*, 1205-1209, Acapulco, 2003.

[7] Y. Yin, R. Zane, J. Glaser and R. W. Erickson, "Small-signal analysis of frequency based electronic ballasts", *IEEE Trans Circuits and Systems*, 50, 8, 1103-1110, 2003.

[8] J. A. Oliver, C. Fernandez, R, Prieto and S. A. Cobos, "Circuit oriented model of rectifiers for large signal envelope simulation", *IEEE Power Electronics Specialists Conference, PESC-2005*, 2771-2776, Recife, 2005.

[9] S. Ben-Yaakov and M. M Peretz, "Simulation Bits©: Some less familiar features of PSpice", *IEEE Power Electronics Society Newsletter*, Second Quarter, 16-18, 2005.

[10] S. Ben-Yaakov and N. Krihely, "Modeling and driving piezoelectric resonant blade elements", *IEEE Applied Power Electronics Conference, APEC-2004*, 1733-1739, Anaheim, 2004.

[11] Cadence Design Systems, Inc., "PSpice optimizer user's guide", 2nd edition, 2000.

[12] E. Deng and S. C'uk, "Negative incremental impedance and stability of fluorescent lamp", *IEEE Applied Power Electronics Conference, APEC'97*, pp. 1050–1056, Atlanta, 1997.

[13] E. Deng, "Negative incremental impedance of fluorescent lamp", Ph. D. dissertation, California Institute of Technology, Pasadena, 1995.

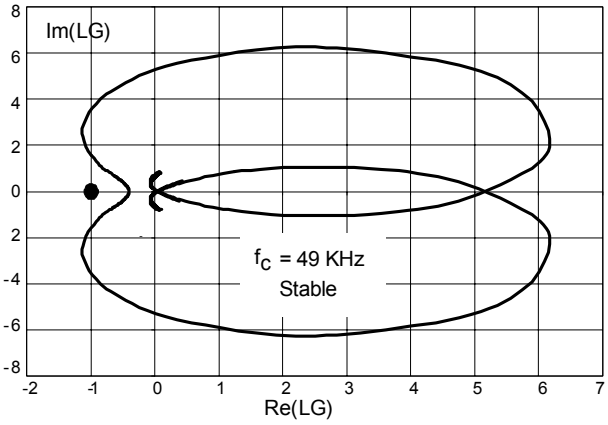

(a)

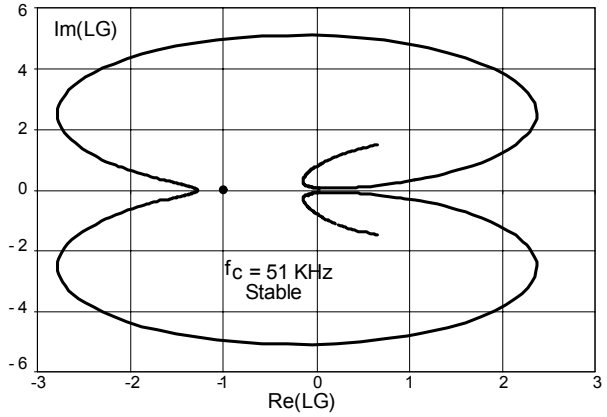

(b)

Figure 18. Typical Nyquist plots of experimental PT-CCFL system: (a) carrier frequency is far from resonance, stable operation. and (b) carrier frequency near resonance, unstable operation.